

## A7.3 Defects in GaN and related materials: perfect dislocations, partial dislocations, dislocation movement and cracks

L.T. Romano

August 1998

### A INTRODUCTION

Edge, screw and mixed dislocations are formed in GaN by dislocation reactions and/or the coalescence of islands during growth [1-4]. Typical dislocation densities in GaN films grown on sapphire or SiC range from  $10^8$  to  $10^{10}$  threading dislocations  $\text{cm}^{-2}$  [1-5]. The lowest threading defect density for GaN films grown on sapphire has been reported to be mid- $10^6$  dislocations  $\text{cm}^{-2}$  for thick films ( $>300\text{ }\mu\text{m}$ ) grown by HVPE [6]. Dislocation mobilities are expected to be lower (at a given temperature) in GaN-based materials compared to GaAs and GaP-based materials because of the larger bond energies in the nitride materials [7,8]. The orientation of the slip plane with respect to the growth direction [9] is also a factor affecting dislocation mobility. The low dislocation mobility may lead to crack formation in GaN at high doping and alloy concentrations.

### B PERFECT DISLOCATIONS

A dislocation is a line defect that is defined by its Burgers vector  $\mathbf{b}$  and line direction  $\xi$ . The Burgers vector describes the lattice displacement for the dislocation within the crystal. For a perfect dislocation  $\mathbf{b}$  is equivalent to a unit lattice vector. FIGURES 1(a) and 1(b) are schematics showing the dislocation lines, Burgers vectors and crystal notation used for the relevant defects in the wurtzite crystal structure. The dislocation line may be defined as a line that forms a boundary between the sheared and unsheared parts of the slip plane in the crystal [9]. The dislocation is an edge defect if  $\mathbf{b}$  and  $\xi$  are perpendicular, whereas it is a screw defect if these vectors are parallel. A mixed dislocation has both an edge and screw component, i.e. the angle between  $\mathbf{b}$  and  $\xi$  is between zero and 90 degrees. Edge, screw and mixed perfect dislocations are all present in wurtzite GaN with  $\mathbf{b} = 1/3\langle 11\bar{2}0 \rangle$ ,  $\langle 0001 \rangle$  or  $1/3\langle 11\bar{2}3 \rangle$  [1-5]. Note that  $\mathbf{b}$  depends on the crystallography (see FIGURE 1), whereas the dislocation line can be along any direction in the crystal. However for GaN on c-plane sapphire, the most common dislocations are those with  $\xi$  parallel to the  $[0001]$  growth direction [1-5]. The movement of dislocations occurs along the slip planes. Slip generally occurs on planes with the highest atomic density. For the wurtzite crystal structure, slip is most frequently observed on the  $\{0001\}$  basal plane for dislocations with  $\mathbf{b} = 1/3\langle 11\bar{2}0 \rangle$  [9]. (However in GaN, dislocation movement seems to be negligible, and instead, cracking occurs for reasons discussed in Sections D and E below.)

The relative concentrations of the various types of dislocations present in GaN depend on the growth parameters. Heying and co-workers demonstrated that the ratio of mixed to edge dislocations was dependent on the conditions during the initial stages of MOCVD growth [10]. Screw dislocations ( $\mathbf{b} = \langle 0001 \rangle$ ) constitute a relatively small fraction of the dislocations present under most growth conditions [1-5,11-13]. Their origin is not established, but they may form as a result of islands forming at steps on the sapphire substrate [13,14]. The presence of more mixed-type dislocations seems to correlate with a lower total defect density (mid- $10^8$  dislocations  $\text{cm}^{-2}$ ) [3,4]. In films with a defect density of  $\sim 10^{10}$  dislocations  $\text{cm}^{-2}$ , the threading dislocations are predominately edge-type [1,10]. For films with a defect density of mid- $10^8$  dislocations  $\text{cm}^{-2}$ , grown by MOCVD, the ratio of mixed to edge dislocations was also found to change with film thickness [3]. Approximately 40% of the threading dislocations were pure edge for 1  $\mu\text{m}$  thick films and  $\sim 70\%$  were pure edge for 5  $\mu\text{m}$  thick films [3]. Edge dislocations are associated with the coalescence of slightly misoriented islands [1-3,11,12],

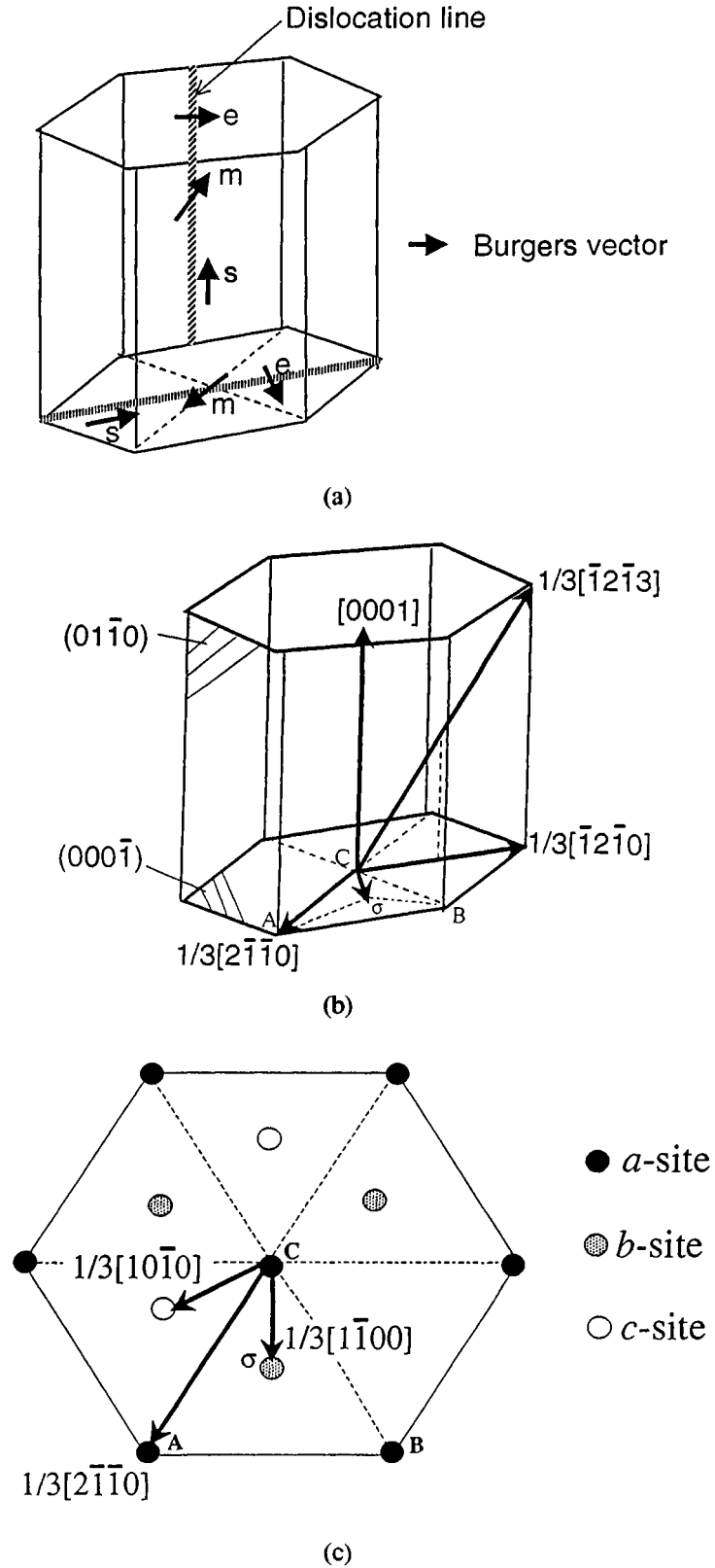


FIGURE 1 (a) Schematic diagram of the hexagonal unit cell showing the relationship between a threading dislocation along the  $[0001]$  direction and an interfacial dislocation in the  $(0001)$  basal plane with their Burgers vectors. The Burgers vectors shown are either edge ( $e$ ), screw ( $s$ ) or mixed ( $m$ ). (b) The crystallographic notation for directions in the hexagonal structure. (c) Schematic of Burgers vectors for Shockley partial dislocations on the  $(0001)$  basal plane.

whereas mixed character dislocations ( $\mathbf{b} = 1/3\langle 11\bar{2}3 \rangle$ ) are formed within individual islands [11]. Mixed dislocations can form through a reaction between dislocations with  $\mathbf{b} = 1/3\langle 11\bar{2}0 \rangle$  and  $\langle 0001 \rangle$ . This has been observed in films grown by MOCVD on  $\text{Al}_2\text{O}_3$  (0001) [3] and 6H-SiC [13]. However, this reaction was not observed for films grown by HVPE even though ~50% of the dislocations had  $\mathbf{b} = 1/3\langle 11\bar{2}3 \rangle$  [4]. Instead, the reaction of partial dislocations associated with the stacking fault defects at the film/substrate interface could explain a high density of mixed dislocations, as discussed below.

## C PARTIAL DISLOCATIONS

Since the energy per unit length of a dislocation is proportional to the square of the magnitude of  $\mathbf{b}$  [9], it can be energetically favourable for a perfect dislocation to split into partial dislocations and form a stacking fault or stacking loop. The Burgers vector of the partial dislocation,  $\mathbf{b}^p$ , is then smaller than a unit lattice vector. A Shockley partial dislocation is in the same plane as the slip plane of the crystal whereas a Frank partial dislocation is normal to the slip plane. FIGURE 1(c) schematically illustrates Shockley partial dislocations in the (0001) basal plane of a hexagonal crystal. The a, b, and c-sites represent the three sets of possible lattice sites in a zincblende or wurtzite crystal structure. For the wurtzite crystal structure, the c-site is not occupied unless a lattice displacement occurs (refer to Datareview A7.2). This displacement is described by a partial dislocation with  $\mathbf{b}^p = 1/3[10\bar{1}0]$  or  $1/3[1100]$ . A sum of these partial dislocations is equal to a perfect dislocation with  $\mathbf{b} = 1/3[2\bar{1}10]$ . TABLE 1 lists the perfect and partial dislocations in the hexagonal crystal structure and their energy per unit length determined from the magnitude of  $\mathbf{b}$  [9].

TABLE 1 Perfect and partial dislocations in the hexagonal crystal structure and their energy per unit length which is proportional to  $|\mathbf{b}|^2$ . This assumes a perfect hexagonal lattice where  $c/a = (8/3)^{1/2}$ .

Burgers vector, $\mathbf{b}$	$ \mathbf{b} ^2$	Dislocation type
$1/3[11\bar{2}0]$	$a^2$	Perfect
$[0001]$	$c^2 = (8/3)a^2$	Perfect
$1/3[11\bar{2}3]$	$a^2 + c^2 = (11/3)a^2$	Perfect
$1/3[01\bar{1}0]$	$a^2/3$	Shockley partial
$1/2[0001]$	$c^2/4 = (2/3)a^2$	Frank partial
$1/6[02\bar{2}3]$	$a^2$	Frank partial

The reaction of partial dislocations to form perfect dislocations is also possible [15]. FIGURE 2(a) shows a high magnification transmission electron microscopy (TEM) image of partial dislocations associated with basal plane stacking faults near the interface of a GaN film grown on sapphire by HVPE. The stacking faults are found to be discontinuous and appear to form boundaries (arrows in FIGURE 2(a)). A low magnification image through a thicker region of the same sample is shown in FIGURE 2(b). The individual partial dislocations associated with the stacking faults cannot be resolved; however, a mixed dislocation with  $\mathbf{b} = 1/3\langle 21\bar{1}3 \rangle$  is visible at the intersection of a boundary similar to the one indicated in FIGURE 2(a). It is possible that this dislocation may have formed from the reaction of two partial dislocations on the prism planes, i.e.  $1/6\langle 20\bar{2}3 \rangle + 1/6\langle 2\bar{2}03 \rangle = 1/3\langle 21\bar{1}3 \rangle$  [4].

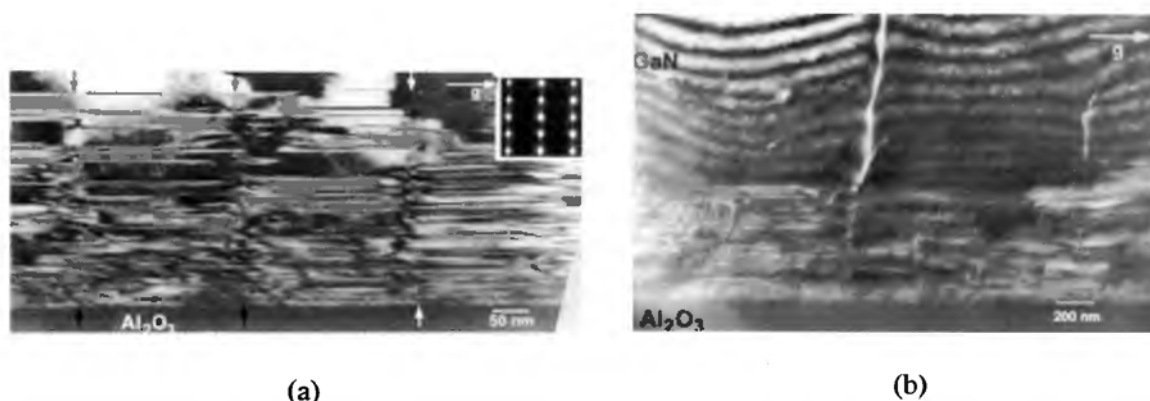


FIGURE 2 (a) Cross-section TEM micrograph of basal plane partial dislocations associated with stacking faults at the interface of a GaN film grown on sapphire (0001) by HVPE: arrows indicate the position of boundaries where the faults are discontinuous. (b) A lower magnification image of a thicker region of the same sample near the film/substrate interface. A mixed dislocation is present at the same type of boundary shown in (a). Both images are taken near the  $[11\bar{2}0]$  axis with  $g = 1100$  [4].

## D DISLOCATION MOVEMENT

Dislocation mobility in GaN appears to be negligible under the growth conditions reported in the literature. The growth of GaN along the  $[0001]$  direction may account for the difficulty in dislocation mobility due to the relationship of the stress in the film and the easy glide systems. The formation and movement of dislocations depends on the critical resolved shear stress on preferred crystallographic slip systems [9]. The most favoured slip systems in the wurtzite crystal structure are dislocations with  $b = \langle 11\bar{2}0 \rangle$  on the  $\{0001\}$  basal planes followed by slip on the  $\{10\bar{1}0\}$  prism planes [9]. Stresses in films generally arise from a film/substrate chemical/lattice mismatch or thermal mismatch [15]. These stresses are biaxial and therefore parallel to the interface [16]. Consequently, the resolved shear on the  $(0001)$  basal planes and the  $\{10\bar{1}0\}$  prism planes (perpendicular to the interface) is zero. However strain fields associated with dislocations could result in an attraction or repulsion of dislocations depending on the sign of  $b$  [9]. The ease of cross slip of dislocations with a screw component ( $b$  parallel to the dislocation line) on the basal and prism planes, may explain defect reduction for these types of defects observed in films grown by MOCVD [17].

Recently, Sugiura [18,19] has attempted to calculate the dislocation mobility in GaN-based materials by comparing to AlGaAs/GaAs and InGaAsP/InP materials. The activation energy of dislocation motion was correlated to the bond strength, which is greater in GaN than in GaAs [7,8]. This resulted in dislocation glide velocities that were approximately a factor of  $10^{11} - 10^{14}$  lower than in InGaAsP and AlGaAs respectively [18,19].

## E CRACKS

Although cracking is often observed in GaN epitaxial films, there have been very few publications on this subject [20,21]. Hiramatsu and co-workers studied residual stress in thick GaN films grown by HVPE [21]. For films  $< 4 \mu\text{m}$  thick, compressive strain was observed in the films by an increase in the  $c$  lattice constant. However for films  $4 - 20 \mu\text{m}$  thick, microcracks were observed near the film/substrate interface [21]. Nakamura has suggested that a  $0.1 \mu\text{m}$  thick  $\text{In}_{0.05}\text{Ga}_{0.95}\text{N}$  layer below the AlGaIn clad layer in laser devices is needed to suppress cracking in nitride films [22].

## REFERENCES

- [1] W. Qian, M. Skowronski, M.D. De Graef, K. Doverspike, L.B. Rowland, D.K. Gaskill [ *Appl. Phys. Lett. (USA)* vol.66 (1995) p.1252 ]
- [2] X.J. Ning, F.R. Chien, P. Pirouz, J.W. Yang, M. Asif Khan [ *J. Mater. Res. (USA)* vol.11 (1996) p.580 ]
- [3] X.H. Wu et al [ *J. Appl. Phys. (USA)* vol.80 (1996) p.3228 ]
- [4] L.T. Romano, B.S. Krusor, R.J. Molnar [ *Appl. Phys. Lett. (USA)* vol.71 (1997) p.2283 ]
- [5] R.C. Powell, N.-E. Lee, Y.-W. Kim, J.E. Greene [ *J. Appl. Phys. (USA)* vol.73 (1993) p.203 ]
- [6] R.P. Vaudo, V.M. Phanse, X.H. Wu, Y. Golan, J.S. Speck [ *Appl. Phys. Lett. (USA)* (1998) ]
- [7] W.A. Harrison [ in *Electronic Structure and Properties of Solids* (Freeman, San Francisco, 1980) ]
- [8] J.E. Northrup, J. Neugebauer [ *Phys. Rev. B (USA)* vol.53 (1996) p.R10477 ]
- [9] J. Hirth, J. Lothe [ in *Theory of Dislocations* (John Wiley & Sons, New York, 1982) ]
- [10] B. Heying et al [ *Appl. Phys. Lett. (USA)* vol.68 (1996) p.643 ]
- [11] X.H. Wu et al [ *Jpn. J. Appl. Phys. (Japan)* vol.35 (1996) p.L1648 ]
- [12] P. Vennegues, B. Beaumont, M. Vaille, P. Gibart [ *J. Cryst. Growth (Netherlands)* vol.173 (1997) p.249 ]
- [13] F.R. Chien, X.J. Ning, S. Stemmer, P. Pirouz, M.D. Bremser, R.F. Davis [ *Appl. Phys. Lett. (USA)* vol.68 (1996) p.2678 ]
- [14] D. Cherns, W.T. Young, J.W. Steeds, F.A. Ponce, S. Nakamura [ *J. Cryst. Growth (Netherlands)* vol.178 (1997) p.201 ]
- [15] Y.A. Osipyan, I.S. Smirnova [ *J. Phys. Chem. Solids (UK)* vol.32 (1971) p.1521 ]
- [16] J.W. Matthews [ *J. Vac. Sci. Technol. (USA)* vol.12 (1975) p.126 ]
- [17] D. Kapolnek et al [ *Appl. Phys. Lett. (USA)* vol.67 (1995) p.1541 ]
- [18] L. Sugiura [ *J. Appl. Phys. (USA)* vol.81 (1998) p.1633 ]
- [19] L. Sugiura [ *Appl. Phys. Lett. (USA)* vol.70 (1998) p.1317 ]
- [20] N. Itoh, J.C. Rhee [ *J. Appl. Phys. (USA)* vol.58 (1985) p.1828 ]
- [21] K. Hiramatsu, T. Detchprohm, I. Akasaki [ *Jpn. J. Appl. Phys. (Japan)* vol.32 (1993) p.1528 ]
- [22] S. Nakamura [ *J. Cryst. Growth (Netherlands)* vol.170 (1997) p.11 ]